

Supporting Information

Engineering Hepatitis B Virus Core Particles for Targeting HER2 Receptors *In Vitro* and *In Vivo*

Izzat Fahimuddin Bin Mohamed Suffian¹, Julie Tzu-Wen Wang¹, Naomi O. Hodgins¹, Rebecca Klippstein Martin¹, Mitla Garcia-Maya², Paul Brown², Yuya Nishimura³, Hamed Heidari⁴, Sara Bals⁴, Jane Sosabowski⁵, Chiaki Ogino³, Akihiko Kondo³, Khuloud T. Al-Jamal^{1}*

¹ *Institute of Pharmaceutical Science, King's College London, Franklin-Wilkins Building, 150 Stamford Street, London SE1 9NH, UK.*

² *Randall Division of Cell & Molecular Biophysics, King's College London, New Hunt's House, London SE1 1UL, UK.*

³ *Department of Chemical Science and Engineering, Graduate School of Engineering, Kobe University, 1-1 Rokkodai, Nada, Kobe 657-8501, Japan.*

⁴ *Electron Microscopy for Materials Science (EMAT), University of Antwerp, Groenenborgerlaan 171, B-2020, Antwerp, Belgium.*

⁵ *Centre for Molecular Oncology, Bart's Cancer Institute, Queen Mary University of London, London, EC1M 6BQ, UK*

* Corresponding author

Prof. Khuloud T. Al-Jamal

Institute of Pharmaceutical Science, King's College London, Franklin-Wilkins Building,
150 Stamford Street, London SE1 9NH, UK.

Tel: +44(0)20-7848-4525

1. Supporting Materials

Ampicillin sodium, AIM-terrific broth base including trace elements, Tris base Ultra-Pure, EDTA disodium and DTT dithiothreitol were obtained from ForMedium™ (UK). Calcium chloride (anhydrous) and urea (carbamide) were obtained from Melford (UK). Imidazole, Glycerol, 2-mercapoethanol, *N, N, N', N'*-tetramethylethylenediamine, sodium chloride, agarose, ribonuclease A (from bovine pancreas) and Bromophenol Blue sodium salt were obtained from Sigma Life Science (UK). cOmplete™ ULTRA Tablets, glass vials Protease Inhibitor Cocktail and cOmplete™ His-Tag Purification Resin were from Roche (Germany). Sodium hydrochloride and methanol were obtained from Fisher Scientific (UK). Acetic acid ≥99.0% (T) and skimmed milk powder were obtained from Fluka Analytical (Switzerland). Triton® X-100, sodium carbonate, ammonium persulfate and Bovine Serum Albumin lyophilized powder, ≥96% (agarose gel electrophoresis) were obtained from Sigma-Aldrich (Germany). Citric acid monohydrate and Brilliant Blue R were obtained from Sigma (UK). Sodium dodecyl sulphate was obtained from BDH Laboratory (UK). Acrylamide/Bis Solution (30%), 37.5:1, Precision Plus Protein™ Dual Xtra Standards, Precision Protein StrepTactin-HRP Conjugate and Clarity Western ECL Substrate were obtained from Bio-Rad Laboratories (USA). Mouse Anti-Hepatitis B Virus Antibody, core antigen (ayw), clone 10E11 was from Merck Millipore (USA). Hydrochloric acid, for analysis, fuming, 37% solution in water was obtained from Aeros Organic (Germany). UltraPure™ Phenol:Chloroform:Isoamyl Alcohol was obtained from Invitrogen (USA). Anti 6-His affinity purified was obtained from Bethyl Laboratories Inc. (USA). Newborn Calf Serum, Heat Inactivated was obtained from First Link Limited (UK). PE Mouse Anti-Human HER-2/neu and PE Mouse IgG1, κ Isotype Control were from BD Biosciences (USA). Alexa Fluor® 488 NHS Ester (Succinimidyl Ester), MEM GlutaMAX™ Supplement, DMEM high glucose pyruvate, Advanced RPMI 1640 Medium, PBS (10X) pH 7.4, Trypsin-EDTA (0.05%) phenol red, Penicillin-Streptomycin (10,000 U/mL), L-Glutamine (200 mM), GlutaMAX™ Supplement,

SnakeSkin™ Dialysis Tubing 10K MWCO 35 mm and Pierce™ 16% Formaldehyde (w/v) Methanol-free were from Thermo-Fisher Scientific (USA). IsoLink kit was obtained from Mallinckrodt Medical BV (Netherlands). [^{99m}TcCO₄]⁻ solution was obtained from Mallinckrodt Pharmaceuticals (Netherlands). XenoLight™ D-luciferin potassium salt was obtained from Perkin Elmer (EU). *Escherichia Coli*, BL21 (DE3) [F⁻ ompT hsdSB (rB⁻ mB⁻) gal dcm (DE3)] was obtained from Dr. Mitla Garcia Maya, Randall Division of Cell and Molecular Biophysics, King's College London, UK. Plasmids pET-22b(+)-dc183_WT-His6, pET-22b(+)-dc149-His6 and pET-22b(+)-dc149-Z342-His6 were obtained from Associate Professor Chiaki Ogino, Chemical and Science Engineering Department, Kobe University, Japan.

2. Supporting Methods

2.1 Cell culture

A panel of cell lines, of varied degree of HER2 expression, was used in this study. The BT-20 human breast carcinoma (BT-20; ATCC, HTB-19) was cultured in MEM media supplemented with 15% fetal bovine serum (FBS), 50 U/ml penicillin, 50 µg/ml streptomycin, 1% L-glutamine, at 37 °C in 5% CO₂. The IGROV-1 human ovarian adenocarcinoma (IGROV-1; RRID, CVCL_1304) and SKOV-3 human ovary adenocarcinoma (SKOV-3; ATCC, HTB-77) were cultured in DMEM media supplemented with 10% FBS, 50 U/ml penicillin, 50 µg/ml streptomycin, 1% L-glutamine, at 37 °C in 5% CO₂. The HeLa human cervix adenocarcinoma (HeLa; ATCC, CCL-2) were cultured in DMEM media supplemented with 10% FBS, 50 U/ml penicillin, 50 µg/ml streptomycin, 1% L-glutamine, at 37 °C in 5% CO₂. All cells were routinely grown in 75 cm² canted-neck tissue culture flasks and passaged twice a week using Trypsin/EDTA at 80% confluency.

2.2 Determination of HER2 receptors expression levels in cancer cell lines

Cells were cultured in complete media in 25 cm² canted-neck tissue culture flasks. When cells reached 80% confluency, cells were washed twice with PBS buffer; trypsinised and 1 x 10⁶ cells were transferred to assay tubes for the subsequent immunostaining. Cells were fixed in 4 % PFA for 10 min at room temperature, washed in PBS buffer and incubated with 150 µl of blocking buffer (1% BSA in PBS buffer) for 30 min at room temperature. After this period of time, cells were washed with PBS buffer and incubated with 20 µl of PE Mouse Anti-Human HER-2neu antibody (BD Biosciences, USA) or 20 µl of Isotype Mouse BALB/c IgG₁, κ for 30 min in dark at room temperature. Finally, cells were washed with PBS buffer. PE fluorescence was analysed by flow cytometry using a BD FACS Calibur™ flow cytometer (BD Biosciences, USA). A total of 10,000 cells were gated and fluorescence was analysed in triplicates for each condition using the FL-2 detector and BD CellQuest software (BD Biosciences, USA).

3. Supporting Results

3.1 Characterisation of cancer cells for HER2 expression

HER2 expression levels in 9 cancer cell lines, including MDA-MB-468, MDA-MB-231, IGROV-1, HeLa, BT-20, SKOV-3, MDA-MB-435-MLE, SKBR-3 and BT-474 cells, were assessed using flow cytometry. Expression levels were assessed by measuring the median fluorescent intensity (MFI) using FL-2 detector. Cell lines were stained with PE mouse anti-human HER2/neu primary antibody. κ isotype was used as a negative control.

As shown in **Figure S1A**, MDA-MB-468 cells showed no difference in the mean fluorescence intensity (MFI) between cells stained with the mouse anti-human HER2/neu primary antibody and naïve (grey colour) or isotype control cells (green line); suggesting that

MDA-MB-468 cells are HER2 negative. On the contrary, MDA-MB-231, IGROV-1, HeLa, BT-20, SKOV-3, MDA-MB-435-MLE, SKBR-3 and BT-474 were confirmed HER2 positive, as shown by the increase in MFI of cells, stained with mouse anti-human HER2/neu (FL2) (purple line) (**Figure S1A**). Based on MFI values, HER2 expression levels on cells were ranked in the following order: MDA-MB-468 < MDA-MB-231 < IGROV-1 < HeLa < BT-20 < SKOV-3 < MDA-MB-435-MLE < SKBR-3 < BT-474. Cells were classified as negative (-) (MDA-MB-468), lowly expressed (+) (MDA-MB-231, IGROV-1, HeLa, BT-20) or overly expressed (+++) (SKOV-3, MDA-MB-435-MLE, SKBR-3, BT-474) for HER2 receptors (**Figure S1B**). Only MDA-MB-468, MDA-MB-231, SKBR-3 and BT-474 cell lines were chosen as representative cell lines for further cellular uptake studies.

3.2 Fluorescence labelling of HBc particles

All HBc particles were fluorescently labelled with Alexa Fluor™ 488 dye. Fluorescence was measured with excitation at 485 nm and emission at 520 nm, using BMG FLUOstar Omega fluorometer. As shown in **Figure S2**, HBc particles showed higher fluorescence intensity than Δ HBc and Z_{HER2} - Δ HBc particles (**Figure S2**).

3.3 *In vivo* monitoring of highly-expressing HER2 (HER2 (+++)) xenograft tumour models by bioluminescence imaging

In order to study the biodistribution of HBc particles in an *in vivo* model, two tumour mice models were prepared; intraperitoneal and mammary fat pad tumour models. NSG mice were inoculated with luciferase-expressing MDA-MB-435-MLE cells, either intraperitoneally or subcutaneously into the mammary fat pad, to generate intraperitoneal or mammary fat pad tumour models, respectively. Tumour growth in each model was monitored by bioluminescence *in vivo* imaging, every 7 days after inoculation. Ventral images of a representative NSG mouse from both tumour models are shown in **Figure S3**. The

intraperitoneal model showed tumour growths at multiple sites around the abdominal cavity, including the spleen, intestines and male reproductive organs (**Figure S3A**). Meanwhile, localised bioluminescent signals were observed at mammary fat pads on both sides in the mammary fat pad model (**Figure S3B**).

3.4 Blood clearance, excretion profiles and organ biodistribution profile of systemically-administered [$^{99m}\text{Tc}(\text{CO})_3$] $^+$ particles by gamma counting

Blood sampling at early time points demonstrated rapid clearance from the blood with values of $\sim 50\%$ and $\sim 30\%$ ID in blood detected at 30 min-post injection, in intraperitoneal and mammary fat pad tumour models, respectively (**Figure S4A**). At 24 h, these values dropped to $\sim 30\%$ and $\sim 10\%$ ID in blood for intraperitoneal and mammary fat pad tumour models, respectively (**Figure S4A**). High radioactivity eliminated into urine was observed for [$^{99m}\text{Tc}(\text{CO})_3$] $^+$ in both intraperitoneal and mammary fat pad tumour models with $\sim 18\text{-}28\%$ ID eliminated/mouse (**Figure S4B**). A similar excretion profile with HBC particles in faeces was observed for [$^{99m}\text{Tc}(\text{CO})_3$] $^+$ in both models.

[$^{99m}\text{Tc}(\text{CO})_3$] $^+$ was observed to accumulate in multiple organs, with the kidneys ($8.45 \pm 3.53\%$ ID/g) and liver ($8.06 \pm 1.71\%$ ID/g) exhibiting the highest accumulation followed by the intestines ($4.69 \pm 0.29\%$ ID/g), stomach ($4.19 \pm 1.14\%$ ID/g), lungs ($3.40 \pm 1.15\%$ ID/g), spleen ($2.97 \pm 0.28\%$ ID/g) and heart ($1.76 \pm 0.54\%$ ID/g) (**Figure S4C, black bars**). Moreover, tumour accumulation was found to be at $1.44 \pm 0.17\%$ ID/g of tumour (**Figure S4C, black bar**).

[$^{99m}\text{Tc}(\text{CO})_3$] $^+$ showed a similar accumulation profile in systemically-administered mammary fat pad tumour model (**Figure S8C, grey bars**) to that obtained in intraperitoneal model. Tumour uptake was $0.82 \pm 0.20\%$ ID/g of tumour (**Figure S8C, grey bars**).

3.5 *In vivo* whole body SPECT/CT imaging, excretion profiles and organ biodistribution profile of locally-administered [^{99m}Tc(CO)₃]⁺ particles by gamma counting

In intraperitoneal tumour-bearing mice, whole body SPECT/CT imaging of [^{99m}Tc(CO)₃]⁺ exhibited a different profile to the HBc particles, in which, an intense radioactivity signals were observed in heart, lungs, liver and bladder. [^{99m}Tc(CO)₃]⁺ signals were mostly cleared at 24 h post-injection (**Figure S5A**). Meanwhile, the excretion profile exhibited low radioactivity eliminated in urine ($3.17 \pm 0.14\%$ ID eliminated/mouse) and faeces ($0.65 \pm 0.83\%$ ID eliminated/mouse) for [^{99m}Tc(CO)₃]⁺ (**Figure S5B**). Very low organ accumulation was observed with the uptake of [^{99m}Tc(CO)₃]⁺ in the intestines ($3.55 \pm 1.89\%$ ID/g), followed by the liver ($2.49 \pm 0.39\%$ ID/g), kidneys ($2.38 \pm 0.13\%$ ID/g), stomach ($2.29 \pm 1.02\%$ ID/g) and spleen ($1.14 \pm 0.46\%$ ID/g) (**Figure S5C**). A relatively low tumour accumulation of [^{99m}Tc(CO)₃]⁺ ($2.32 \pm 0.84\%$ ID/g) was observed (**Figure S5C**).

In the whole body SPECT/CT imaging of mammary fat pad tumour-bearing mice, [^{99m}Tc(CO)₃]⁺ exhibited a similar biodistribution profile to ^{99m}Tc-ΔHBc and ^{99m}Tc-Z_{HER2}-ΔHBc, where by most of the signals were retained in the tumour (**Figure S6A**). No significant radioactivity signals were observed in any organs except bladder, which indicated that some of the particles reached the systemic circulation prior to elimination in the urine. As shown in **Figure S6B**, [^{99m}Tc(CO)₃]⁺ also resulted in a similar excretion profile to HBc particles, with $33.38 \pm 5.66\%$ and $1.36 \pm 0.11\%$ ID eliminated/mouse in the urine and faeces, respectively. Organ accumulation of [^{99m}Tc(CO)₃]⁺ was highest in kidneys, followed by liver and spleen with 14.49 ± 3.55 , 11.46 ± 3.28 and $3.49 \pm 0.37\%$ ID/g of tissue at 24 h post-injection, respectively (**Figure S6C**). [^{99m}Tc(CO)₃]⁺ exhibited high tumour uptake of $\sim 34.77 \pm 15.70\%$ ID/g (**Figure S6C**).

3.6 Blood clearance, excretion profiles and organ biodistribution profile of systemically-administered HBc particles by gamma counting

Quantitative studies by gamma counting were performed to assess the pharmacokinetic profile and organ biodistribution of HBc particles 24 h post-injection. Radiolabelled ^{99m}Tc - ΔHBc and ^{99m}Tc - $\text{Z}_{\text{HER2}}\text{-}\Delta\text{HBc}$ particles were injected *via* the tail vein (systemic route) in both of the tumour models. Blood sampling at early time points demonstrated fast clearance from the blood with values of ~ 7.0 - 7.5% and ~ 4.0 - 5.5% ID in blood detected in blood at 30 min-post injection, in the intraperitoneal (**Figure S7A**) and mammary fat pad (**Figure S7B**) tumour models, respectively. At 24 h, these values dropped to ~ 4.0 - 5.0% and ~ 0.5 - 1.5% ID in blood for the intraperitoneal (**Figure S7A**) and mammary fat pad (**Figure S7B**) tumour models, respectively. No significant difference in the blood clearance profiles between the ^{99m}Tc - ΔHBc and ^{99m}Tc - $\text{Z}_{\text{HER2}}\text{-}\Delta\text{HBc}$ particles was observed. Relatively low levels of radioactivity suggest that both HBc particles have a short blood circulation time in mice. Animals were also housed in metabolic cages for urine and faeces collection for 24 h to assess excretion profile. Approximately ~ 10 - 20% and ~ 1.0 - 2.0% ID was eliminated in urine and faeces within 24 h for both particles ($p > 0.05$) (**Figure S7C, D**).

In the intraperitoneal tumour mouse model, accumulation of ^{99m}Tc - ΔHBc was observed in kidneys $>$ liver $>$ spleen followed by lungs at %ID/g values of 13.90 ± 1.08 , 9.88 ± 1.24 , 9.27 ± 0.57 and $3.41 \pm 0.40\%$ at 24 h post-injection (**Figure S8A, black bars**). A similar trend in organ accumulation profile was observed for ^{99m}Tc - $\text{Z}_{\text{HER2}}\text{-}\Delta\text{HBc}$ (**Figure S8A, grey bars**). The mammary fat pad tumour mouse model exhibited comparable organ biodistribution profiles to those observed in intraperitoneal tumour mouse model (**Figure S8B**). A

statistically significant higher lung (* $p < 0.05$) and lower kidney (** $p < 0.01$) uptakes were observed for $^{99m}\text{Tc-Z}_{\text{HER2}}\text{-}\Delta\text{HBc}$ compared to $^{99m}\text{Tc-}\Delta\text{HBc}$.

Tumour uptake of systemically-administered HBc particles exhibited low uptake with $\sim 0.5\%$ and $\sim 0.2\%$ achieved in the intraperitoneal and mammary fat pad tumour model, respectively, with no significant differences observed between $^{99m}\text{Tc-}\Delta\text{HBc}$ and $^{99m}\text{Tc-Z}_{\text{HER2}}\text{-}\Delta\text{HBc}$ (**Figure S8**).

3.7 Excretion profiles of locally-administered HBc particles by gamma counting

In the intraperitoneal tumour-bearing mice model, approximately $\sim 4\text{-}10\%$ and $\sim 0.2\text{-}2.0\%$ ID was eliminated into urine and faeces after 24 h for both particles with no significant differences between the type of particles ($p > 0.05$) (**Figure S9A**). In contrast, in the mammary fat pad tumour-bearing mice model, higher radioactivity was observed in urine for both HBc particles after 24 h ($\sim 17\text{-}22\%$) than found with the intraperitoneal model. Approximately $\sim 20\text{-}30\%$ and $\sim 1.6\text{-}1.7\%$ ID was eliminated into urine and faeces after 24 h for both particles ($p > 0.05$) (**Figure S9B**).

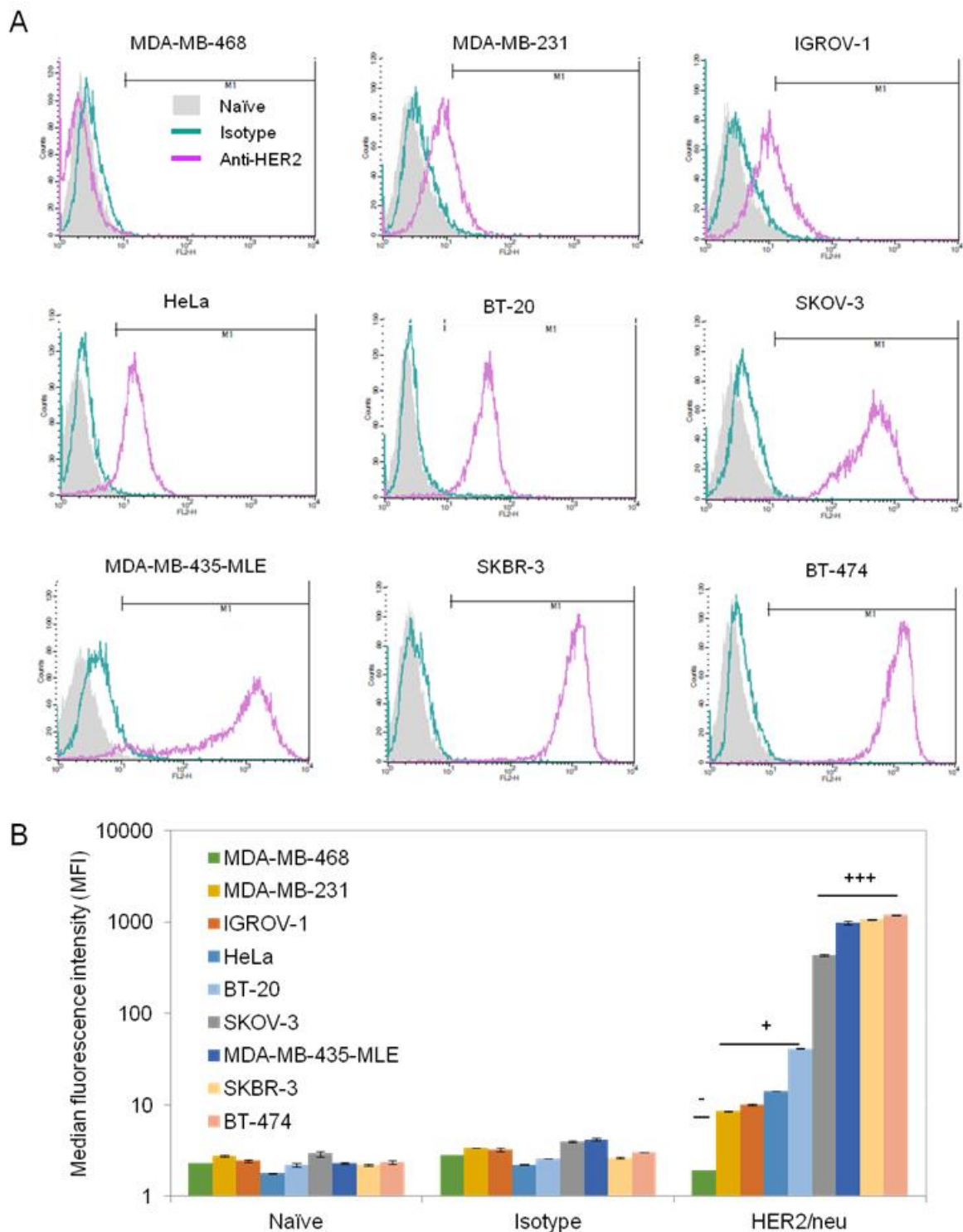


Figure S1. HER2 expression levels in cancer cell lines by flow cytometry. (A) Fluorescence intensity histograms (FL2) and **(B)** Median fluorescence intensity (MFI) analyses. Cell lines were stained with PE mouse anti-human HER2/neu primary antibody for assessing the expression level of HER2 receptors on cell membrane surface. PE mouse anti-human IgG1, κ isotype was used to account for non-specific binding to the IgG. HER2

expression levels on cells are in the following order: MDA-MB-468 > MDA-MB-231 > IGROV-1 > HeLa > BT-20 > SKOV-3 > MDA-MB-435-MLE > SKBR-3 > BT-474. Cells were classified as negative (-), low expression (+) or over-expression (+++) for HER2 receptors.

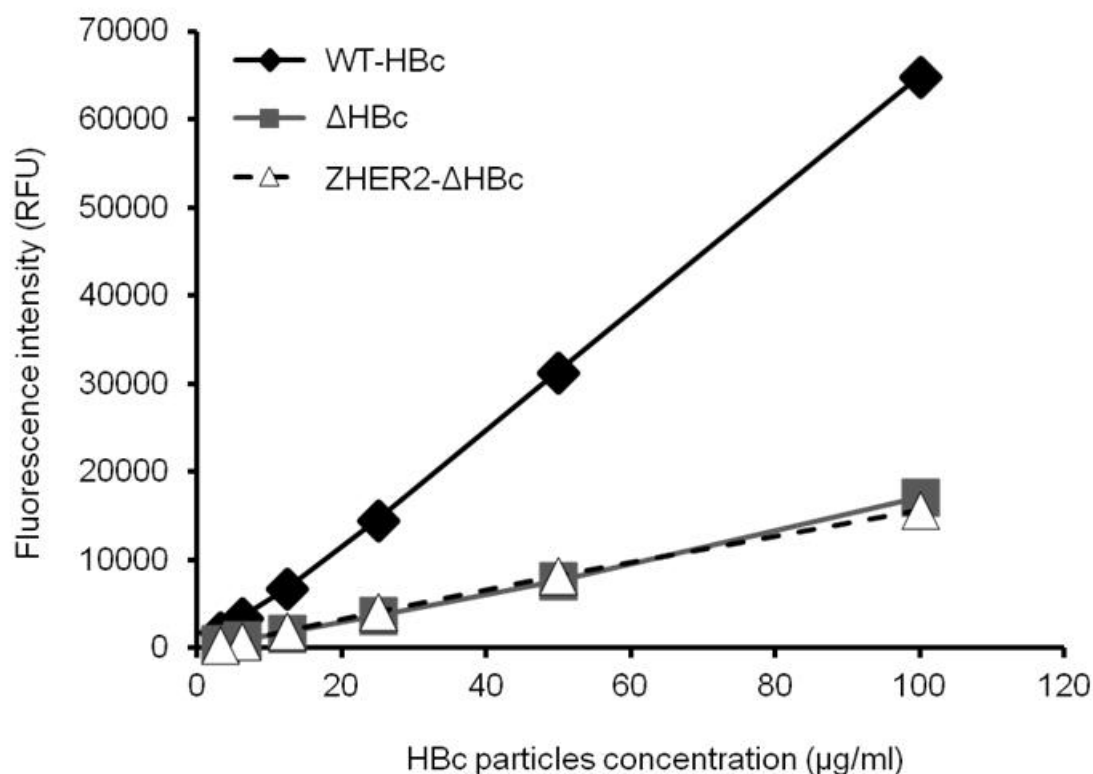


Figure S2. Standard curve of Alexa Fluor™ 488-labelled HBc particles by fluorometry. WT-HBc, Δ HBc and Z_{HER2}- Δ HBc particles were fluorescently labelled with Alexa Fluor™ 488 dye and measured for fluorescence at 485nm and 520 nm excitation and emission wavelengths, respectively. Measurements were performed at 25°C using a BMG FLUOstar Omega fluorometer. Error bars are too small to be seen. Higher labelling efficiency was obtained for WT-HBc than Δ HBc and ZHER2- Δ HBc particles.

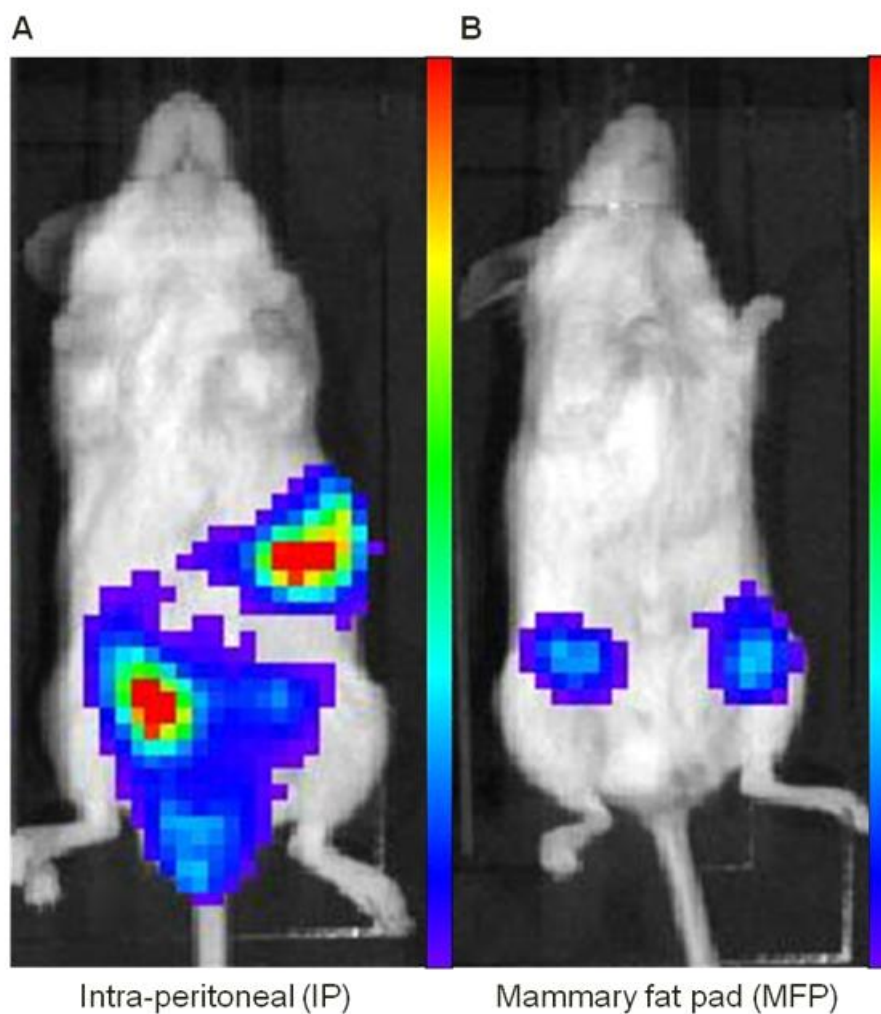


Figure S3. *In vivo* IVIS optical imaging of MDA-MB-435-MLE tumour-bearing NSG mice in different models. NSG mice were inoculated with MDA-MB-435-MLE cells intraperitoneally or subcutaneously to produce (A) intraperitoneal (IP) or (B) mammary fat pad (MFP) tumour bearing mouse model, respectively. Bioluminescence images of mice were captured every 7 days, from day 7 post-inoculation using IVIS Lumina series III *In Vivo* Imaging Device (IVIS). In each imaging session, a total of 150 mg of luciferin per kg body weight was administered *via* subcutaneous injection.

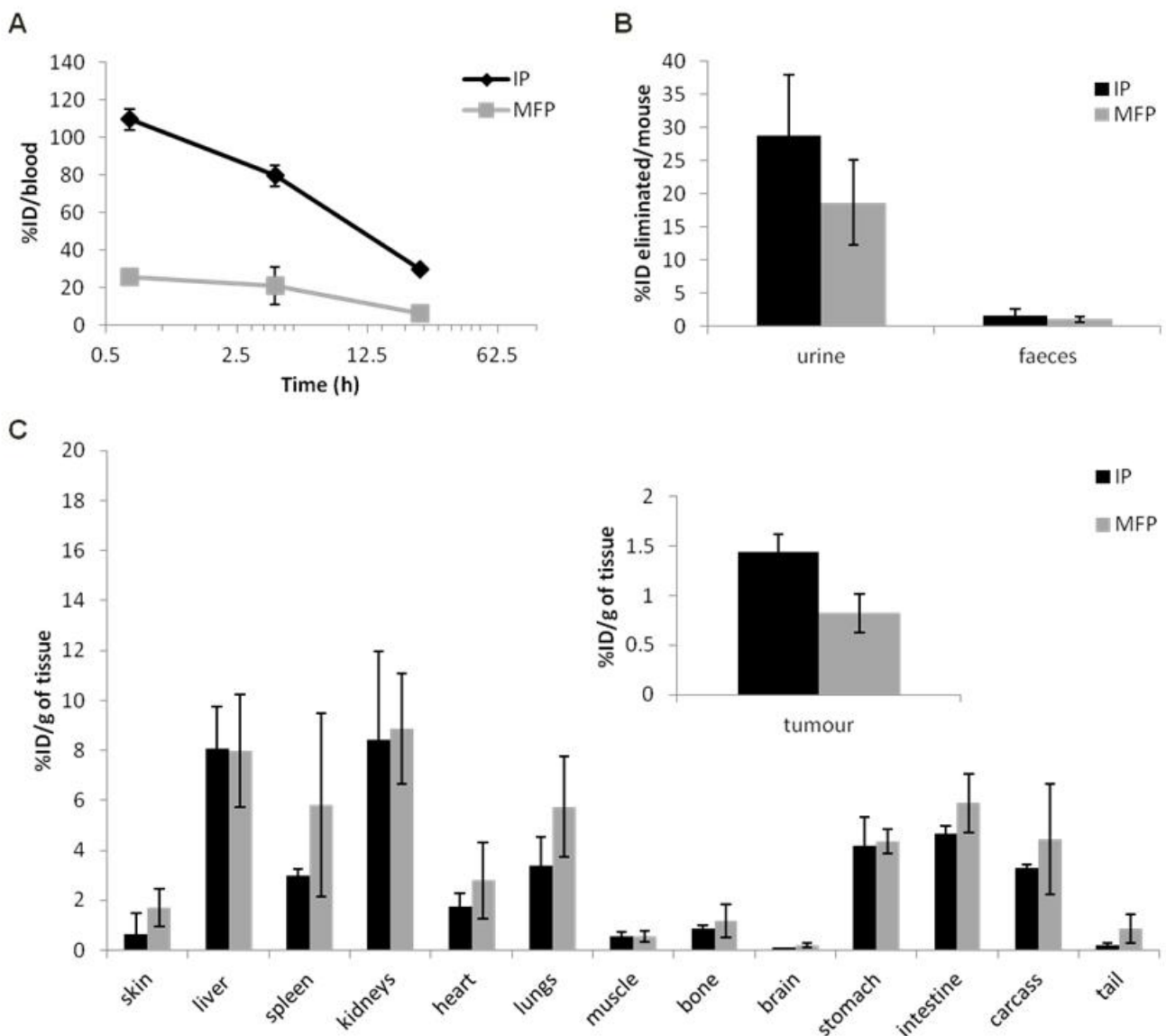


Figure S4. *In vivo* blood circulation, excretion profiles and organ biodistribution of systemically-administered $[^{99m}\text{Tc}(\text{CO})_3]^+$ in MDA-MB-435-MLE IP or MFP tumour-bearing NSG mice. Mice were intravenously injected with $[^{99m}\text{Tc}(\text{CO})_3]^+$ in the IP (black) and MFP (grey) tumour models, at a dose of 6-8 MBq/mouse. **(A)** Blood clearance profiles. Blood samples (5 μl) were collected from the tail vein at 30 min, 4 h and 24 h post-injection. **(B)** Excretion profile at 24 h post injection. **(C)** Organ biodistribution profile with values expressed as %ID/g of tissue; Inset shows the %ID/g tumour uptake. Results are expressed as mean \pm SD (n=3).

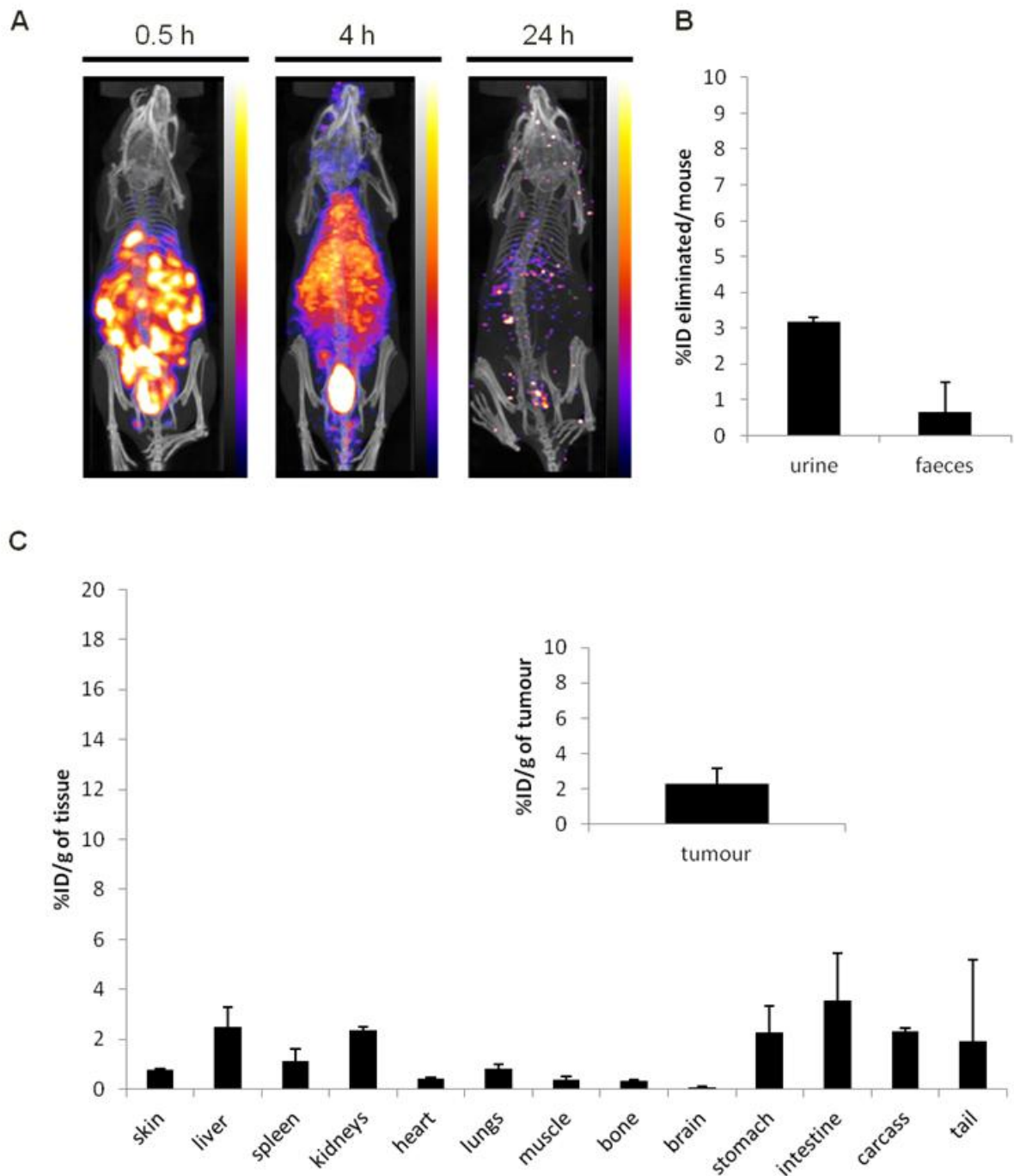


Figure S5. *In vivo* SPECT/CT imaging, excretion profile and organ biodistribution studies of locally-administered $[^{99m}\text{Tc}(\text{CO})_3]^+$ in MDA-MB-435-MLE IP tumour-bearing NSG mice. Mice were intraperitoneally injected at a dose of 6-8 MBq/mouse. Organs were excised at 24 h post-injection for gamma counting. **(A)** Whole body SPECT/CT imaging at 0-30 min, 4 and 24 h post-injection of $[^{99m}\text{Tc}(\text{CO})_3]^+$. **(B)** Excretion profile at 24 h post-injection, expressed as mean of %ID eliminated/mouse \pm SD (n=3). **(C)** Organ biodistribution profile with values expressed as %ID/g of tissue; Inset shows the %ID/g tumour uptake. Results are expressed as mean \pm SD (n=3).

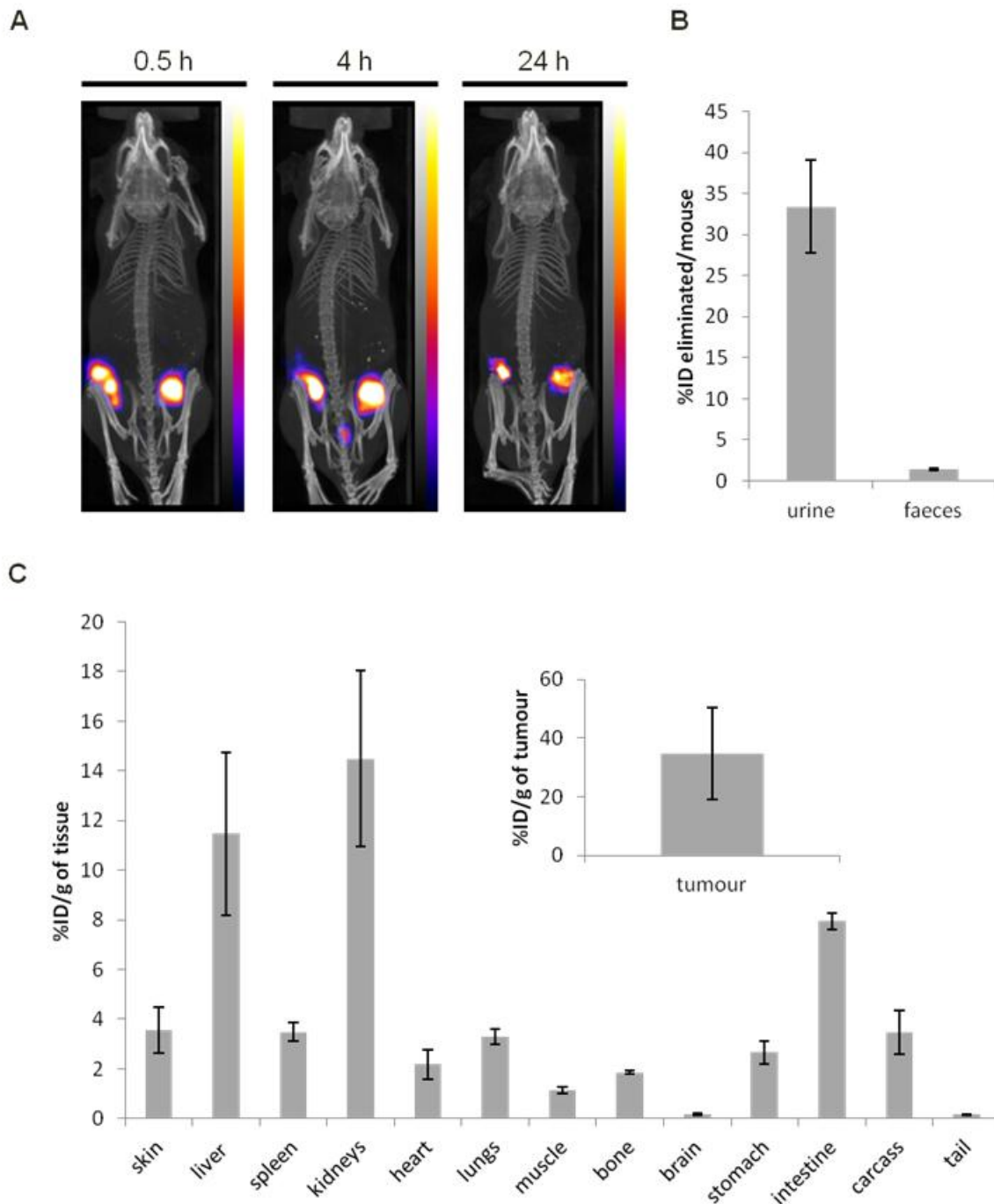


Figure S6. *In vivo* SPECT/CT imaging, excretion profile and organ biodistribution studies of locally-administered $[^{99m}\text{Tc}(\text{CO})_3]^+$ in MDA-MB-435-MLE MFP tumour-bearing NSG mice. Mice were intratumourally injected at a dose of 6-8 MBq/mouse. Organs were excised at 24 h post-injection for gamma counting. **(A)** Whole body SPECT/CT imaging at 0-30 min, 4 and 24 h post-injection of $[^{99m}\text{Tc}(\text{CO})_3]^+$. **(B)** Excretion profile at 24 h post injection, expressed as mean of %ID eliminated/mouse \pm SD (n=3). **(C)** Organ biodistribution profile with values expressed as %ID/g of tissue; Inset shows the %ID/g tumour uptake. Results are expressed as mean \pm SD (n=3).

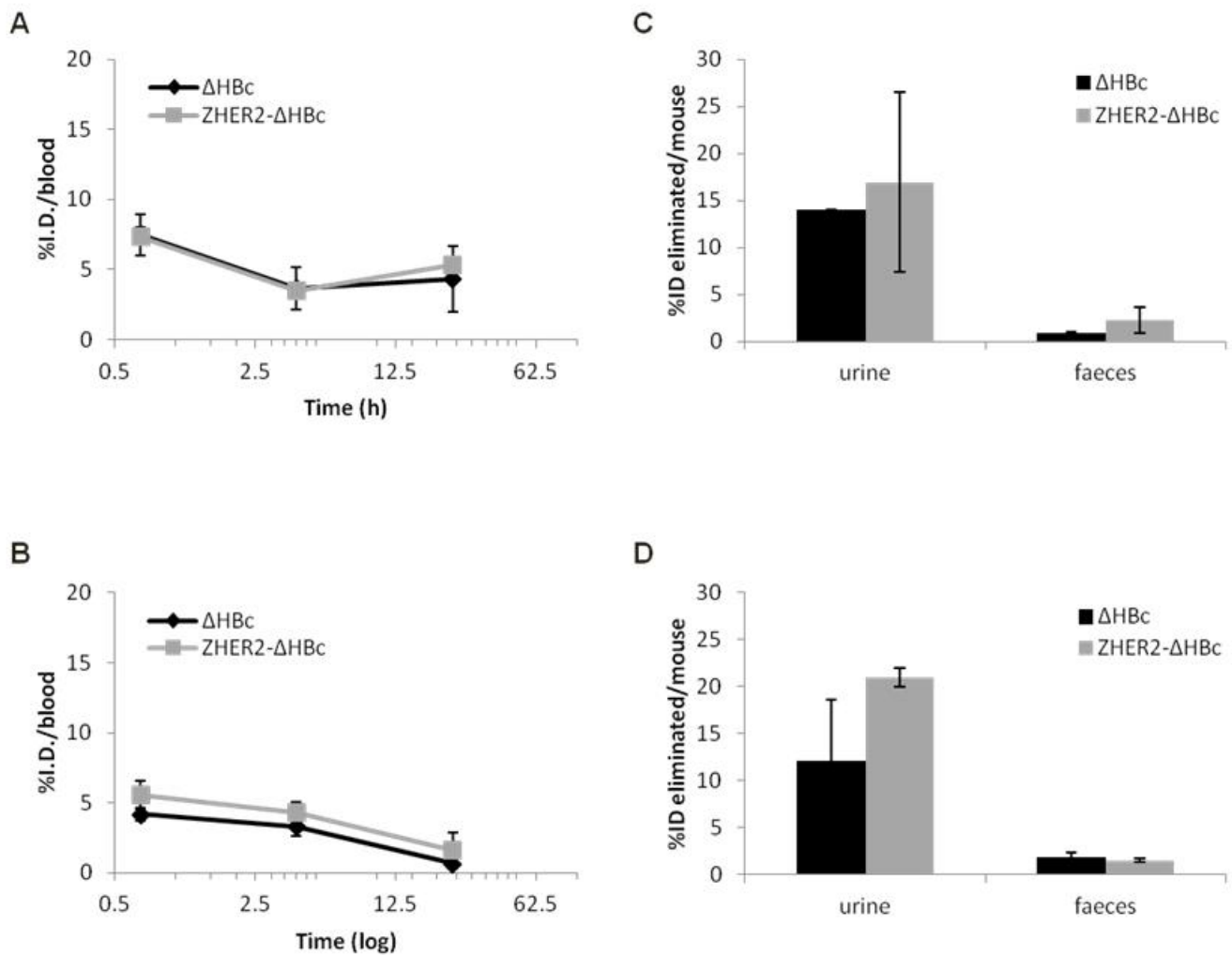


Figure S7. *In vivo* blood circulation and excretion profiles of systemically-administered ^{99m}Tc -HBc particles in IP or MFP model MDA-MB-435-MLE tumour-bearing NSG mice. Mice were intravenously injected with ^{99m}Tc - Δ HBc (black) or ^{99m}Tc -Z_{HER2}- Δ HBc (grey), in the IP (A, C) or MFP (B, D) tumour mouse model, at a dose of 50 μg protein/mouse (4-6 MBq per mouse). (A, B) Blood clearance profiles and (C, D) Excretion profile at 24 h post injection. Blood samples (5 μl) were collected from the tail vein at 30 min, 4 h and 24 h post-injection. Low detection of ^{99m}Tc - Δ HBc or ^{99m}Tc -Z_{HER2}- Δ HBc (2.5-3.0%) was detected in blood at 30 min post-injection or both models. Results are expressed as mean \pm SD (n=3).

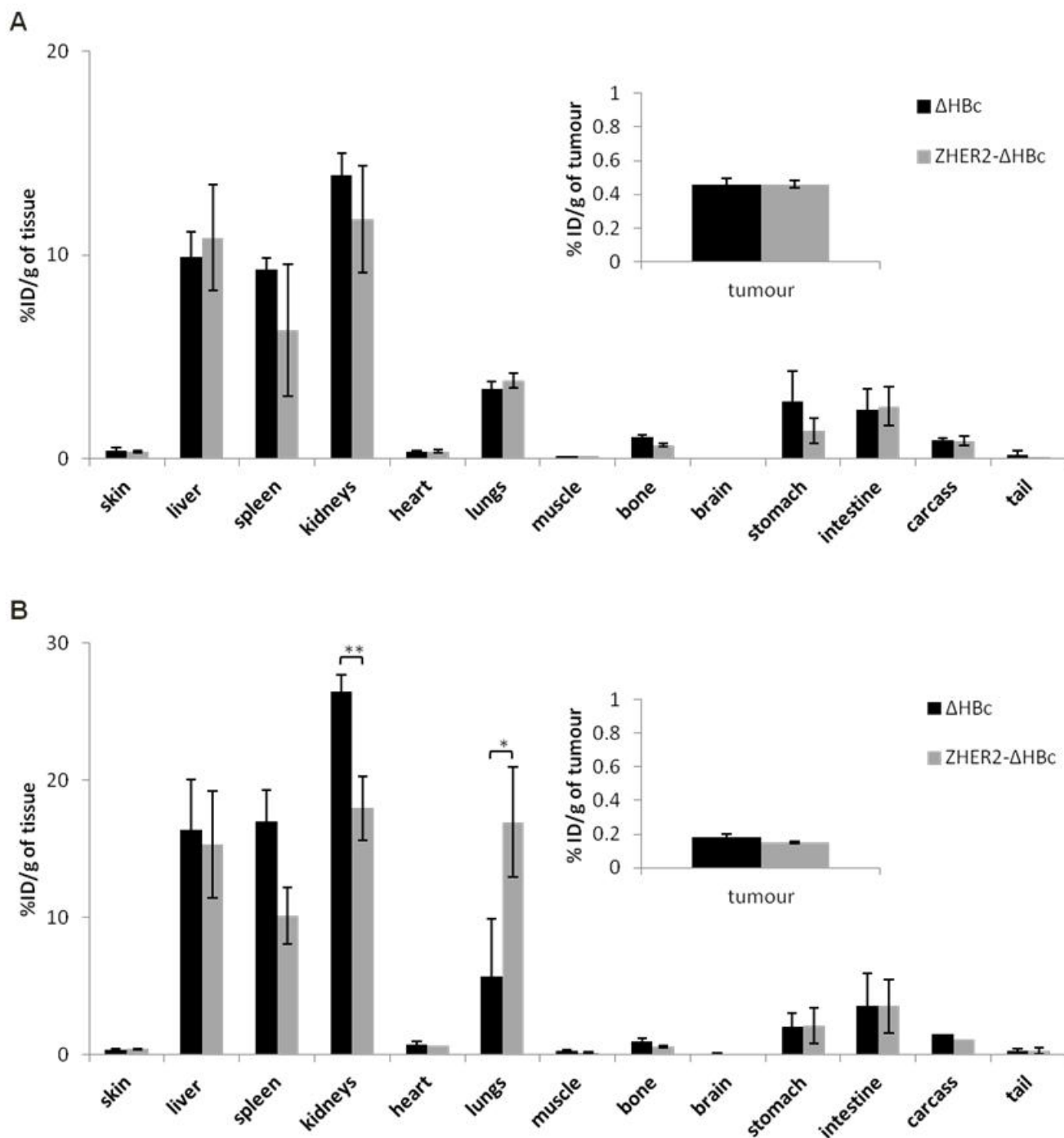


Figure S8. *In vivo* organ biodistribution studies of systemically-administered ^{99m}Tc -HBc particles in IP or MFP MDA-MB-435-MLE tumour-bearing NSG mice. Mice were injected with ^{99m}Tc - Δ HBc (black bars) or ^{99m}Tc -ZHER2- Δ HBc (grey bars), intravenously in the (A) IP or (B) MFP tumour mouse model, at a dose of 50 μg protein/mouse (4-6 MBq per mouse). Organs were excised at 24 h post-injection for gamma counting. Results are expressed as mean of %ID/g of tissue \pm SD (n=3).

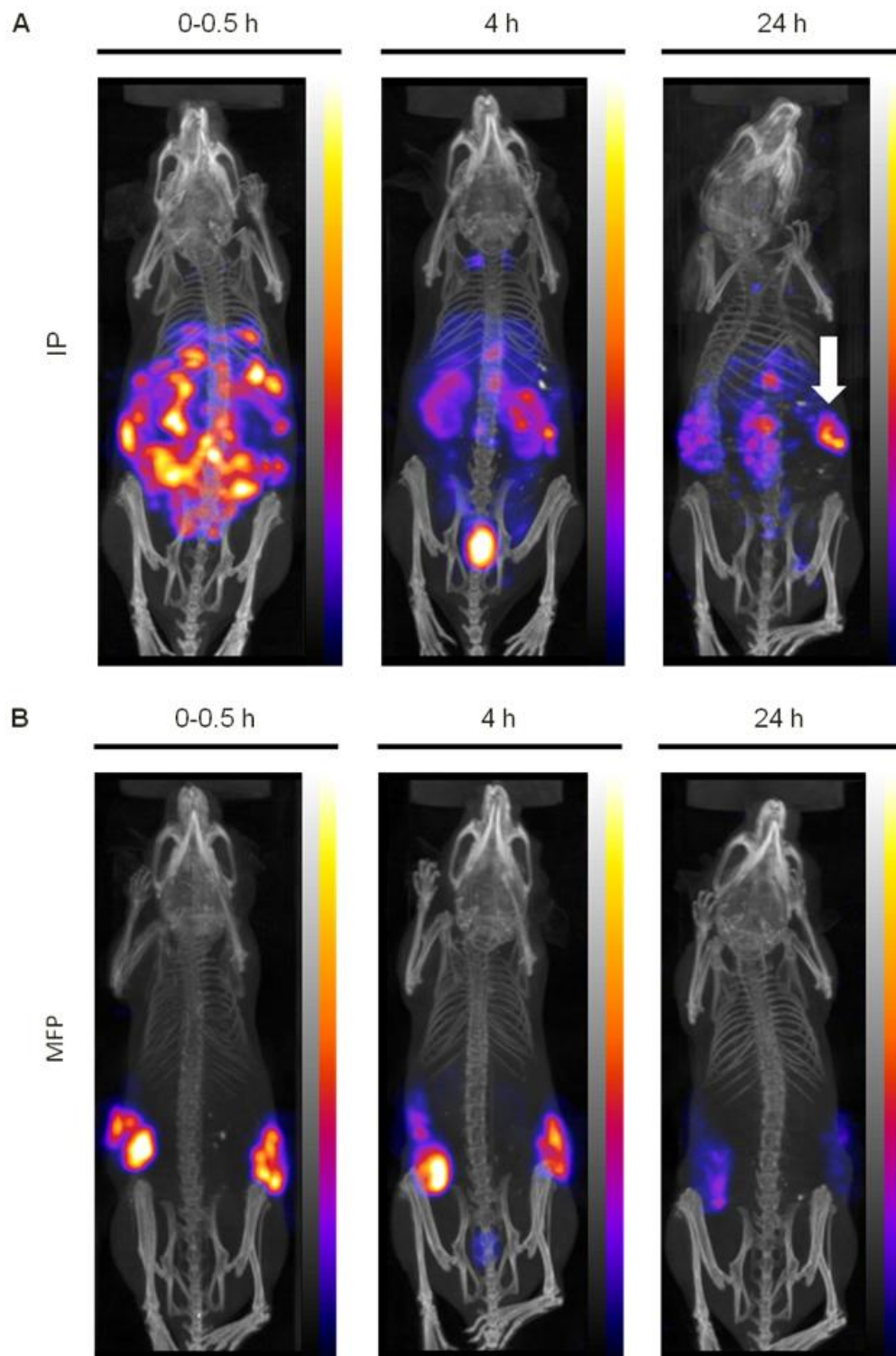


Figure S9. *In vivo* SPECT/CT imaging of ^{99m}Tc - ΔHBc particles in MDA-MB-435-MLE IP and MFP tumour-bearing NSG mice. Mice were injected with ^{99m}Tc - ΔHBc , intraperitoneally, at a dose of 200 μg protein/mouse (6-14 MBq per mouse) in (A) IP or (B) MFP tumour-bearing mice model. Whole body 3D SPECT/CT imaging at 0-0.5, 4 and 24 h post-injection with a scanning time of 30 min each. White arrow indicates accumulation at tumour region at 24 h post-injection.

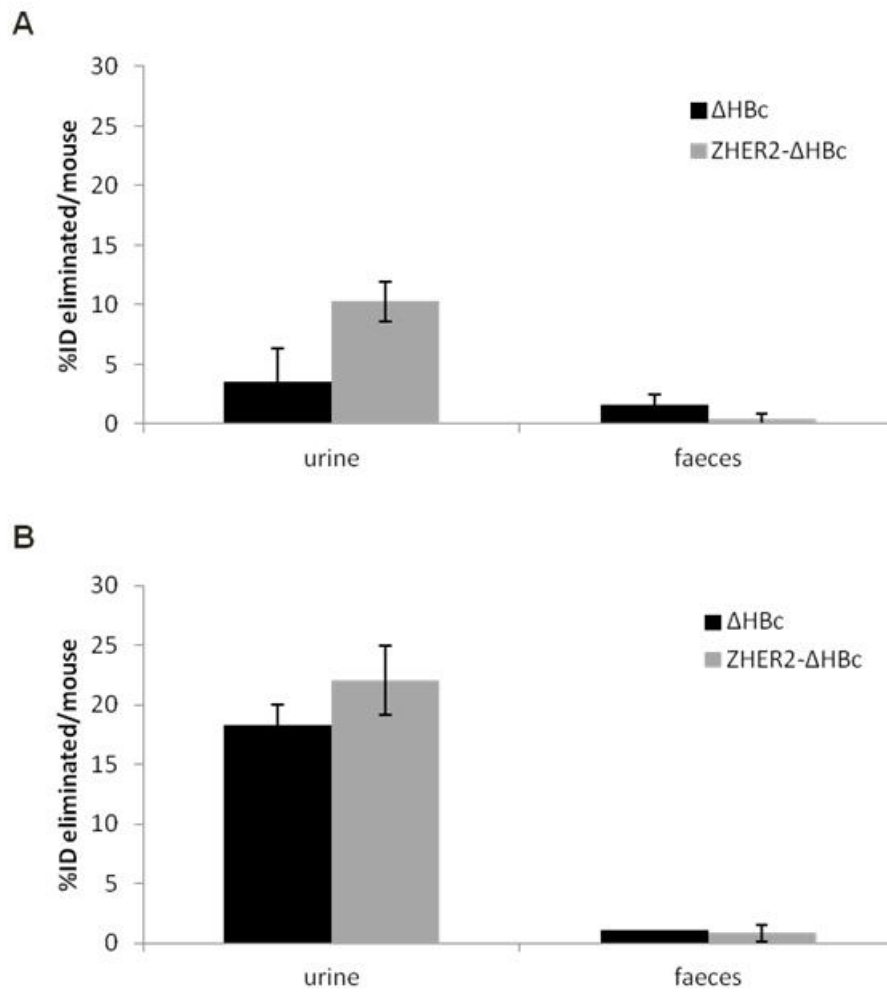


Figure S10. *In vivo* excretion profile of locally-administered [$^{99m}\text{Tc}(\text{CO})_3$] $^+$ in MDA-MB-435-MLE IP or MFP tumour-bearing NSG mice. Mice were injected with ^{99m}Tc - Δ HBc (black bars) or ^{99m}Tc -Z_{HER2}- Δ HBc (grey bars), intraperitoneally or intratumourally in the (A) IP or (B) MFP mouse tumour model, respectively, at a dose of 50 μg protein/mouse (4-6 MBq per mouse). Excretion profile at 24 h post injection is expressed as mean of %ID eliminated/mouse \pm SD (n=3).